JOURNAL OF GEOPHYSICAL RESEARCH, VOL. 90, NO. D1, PAGES 2223-2232, FEBRUARY 20, 1985

CUMULUS CONVECTION AND CLIMATIC TEMPERATURE PERTURBATIONS

Szu-cheng S. Ou and Kuo-Nan Liou

Department of Meteorology, University of Utah, Salt Lake City

Abstract. The influence of cumulus convection on the equilibrium temperature perturbations due to the doubling of CO_2 is investigated by using a one-dimensional radiative-turbulent model. The model includes parameterizations of solar and infrared radiative flux transfer in clear and cloudy conditions, vertical eddy sensible and latent heat fluxes, surface albedo feedback, and an interactive cumulus convection. The cumulus parameterization employed is basically a Kuo-type scheme described and modified by Anthes. In addition the criteria for cumulus convection to take place is derived from values associated with the surface relative humidity and the vertical profile of moist static energy. In the numerical experiments it is found that the extent of condensational heating due to cumulus convection is determined by the depth of the conditionally unstable layer and the total amount of buoyancy force generated by the excess cloud temperature over the surrounding temperature. With the incorporation of cumulus convection, an atmosphere with a high relative humidity will generate a higher temperature near the surface. Also, a higher surface relative humidity will generate a larger upward shift in equilibrium condensational heating rates. Perturbation experiments reveal that the sensitivity of cumulus convection to the surface temperature increase due to doubling of CO_2 is not apparent under mean annual global conditions with a realistic surface relative humidity of 85%. However, with the incorporation of cumulus convection and fixing the horizontal transport of sensible and latent heat fluxes, it is shown that the surface temperature increase in a tropical atmosphere due to doubling of CO_2 significantly reduces from 4.3 to 2.5°K with the upward shift of temperature increases especially evident in upper tropospheric levels. Finally, it is also noted that the tropospheric temperature profile in the tropics generated by the present one-dimensional model with cumulus convection agrees closely with that provided by Oort and Rasmusson for mean annual climatological conditions.

1. Introduction

The effects of radiative cooling and convective heating in the determination of the atmospheric temperature structure have been investigated by means of the so-called convective adjustment first proposed by Manabe and his coworkers [e.g., Manabe and Strickler, 1964; Manabe and Wetherald, 1967] in the context of a one-dimensional thermal equilibrium model. In essence the model simulates the atmospheric convection by adjusting the temperature profile under radiative equilibrium in such a manner that its lapse rate is less than a certain critical value everywhere in the atmosphere, while the total potential energy is conserved. Lindzen et al. [1982] pointed out that the convective adjustment scheme, in general, tends to overestimate the convective heat relase in the lower atmosphere. For this reason they proposed a modification of the radiative-convective model by incorporating a cumulus parameterization scheme.

More recently, Liou and Ou [1983] developed a one-dimensional radiative-turbulent model based on the concept of thermodynamic energy balance between radiative transfer and vertical turbulent heat exchange in which the so-called K theory was utilized to simulate the convective heat transport. The resulting convective heat flux, based on the turbulent theory, depends on the eddy transport coefficient along with temperature and humidity gradients. The eddy transport coefficient generally decreases linearly with increasing height, resulting in a very small heat flux in the upper troposphere. Thus this small heat flux may lead to a significant underestimate of the heat release in a strongly unstable condition. In order to remedy this shortcoming it is necessary to incorporate an appropriate cumulus parameterization scheme to simulate the upward shift of heat exchanges during convective situations.

The concept and theory of cumulus parameterization has been well developed for applications to general circulation and mesoscale models [Kuo, 1965, 1974; Arakawa and Schubert, 1974; Anthes, 1977; Donner et al., 1982]. More recently, Albrecht [1983] has developed a cumulus convection scheme intended for incorporation in climate models based on the principles of Arakawa and Schubert's model. In this paper we wish to investigate the effects of cumulus convection on climatic temperature perturbations utilizing the fundamental one-dimensional radiative-turbulent model developed in our previous paper [Liou and Ou, 1983]. The convective scheme used in the model is adapted from the method presented by Anthes, who modified the basic scheme proposed by Kuo [1974] with simplifications for climatic perturbation experiments. In section 2, we describe some refinements and modifications of the one-dimensional radiative-turbulent model used in temperature perturbation studies. The cumulus convection scheme in conjunction with the present one-dimensional climate model is presented in section 3. Results from the cumulus parameterization scheme and from the coupling between cumulus convection and the radiative-turbulent model in the case of the carbon dioxide greenhouse effect are given in section 4. Finally, conclusions follow in section 5.

Paper number 4D1262.
0148-0227/85/004D-1262$05.00

2. One-Dimensional Radiative-Turbulent Climate Model

In accordance with the analysis presented by Liou and Ou [1983] the basic equation governing the one-dimensional radiative-turbulent climate model may be written in the form

$$\overline{\rho w'(C_p T' + gz' + Lq')} + \int_0^\infty \sigma T^4(z')\, K(|z-z'|)\, dz' = F_S(z) \quad (1)$$

where ρ denotes the density of air, C_p the specific heat at constant pressure, g the gravitational acceleration, L the latent heat of vaporization and condensation, K the IR emissivity kernel, F_S the solar net flux, q the saturation water vapor mixing ratio, and w the vertical velocity.

On utilizing the first-order closure, the K theory, to the thermal eddy flux and adding a countergradient factor γ' to the lapse rate structure to account for steady state and global-scale conditions [Deardorff, 1972], equation (1) may be written in the following form

$$-k_z \rho C_p \left(\frac{\partial T}{\partial z} + \gamma_d - \gamma'\right) + \rho L \overline{w'q'} + \int_0^\infty \sigma T^4(z')\, K(|z-z'|)\, dz' = F_S(z) \quad (2)$$

where k_z represents the eddy thermal diffusion coefficient and γ_d the adiabatic lapse rate. Parameterizations of solar and IR broadband flux transfer under climatic conditions, along with the method of solution to the integro-differential equation using a small perturbation technique, have been documented in our previous papers [Liou and Ou, 1983; Ou and Liou, 1983] and will not be duplicated here. However, we have made a number of physical modifications with respect to the surface flux, humidity, eddy flux, and surface albedo parameterizations in conjunction with the one-dimensional radiative-turbulent model.

2a. Surface Flux

Using the surface flux data presented by Budyko [1982], the sum of the sensible and latent heat fluxes may be correlated with the vertical temperature and humidity gradients in the form

$$H = \overline{\rho w'(C_p T' + Lq')}\Big|_{z\to 0} = C_1 \left[\left|\frac{\partial T}{\partial z}\right| + \frac{L}{C_p}\left|\frac{\partial q}{\partial z}\right|\right]^{C_2} \quad (3)$$

where the empirical constants $C_1 = 37$ and $C_2 = 0.267$ and H is in W m^{-2}. In order to separate the sensible and latent heat fluxes one additional parameter is needed. Based on the approach proposed by Priestley and Taylor [1972] and modified by Peng et al. [1982], the surface latent heat flux LM_t is related to the total flux in the form

$$LM_t = \frac{AH + B}{A + 1} \quad (4)$$

where

$$A = \frac{x}{1 - x} \qquad B = \frac{b\, y}{1 - x}$$

$$x = \frac{a\, y\, \partial q_s(T)/\partial T}{C_p/L + \partial q_s(T)/\partial T}$$

and $a = 0.85$ W m^{-2} and $b = 32.4$ W m^{-2} are empirical constants of correlation between evaporation from a saturated water surface and the equilibrium evaporation that are determined from climatological data, and $y = 0.832$, representing a measure of water available for evaporation over the globe. Using the mean annual surface temperature, we obtain $A = 1.49$ W m^{-2} and $B = 59.36$ W m^{-2}. Consequently, upward latent and sensible heat fluxes can be separated, which is required in the formulation of cumulus convection.

2b. Vertical Eddy Flux

The parameterization of vertical eddy flux is divided into latent and sensible heat transports as illustrated in (2). The eddy thermal diffusion coefficient k_z is determined from a linear interpolation between the surface value and the value at the tropopause [Liou and Ou, 1983]. The second term in (2) represents the latent heat transport, which is parameterized separately according to nonconvective and convective conditions as follows:

$$\rho L \overline{w'q'} = \begin{cases} -k_z' \dfrac{\partial q}{\partial z} & \text{nonconvective} \quad (5a) \\ \dfrac{M_t\, q_c(z)}{q_c(z_b) - q_c(z_t)} - D & \text{convective} \quad (5b) \end{cases}$$

where D is the convective detrainment rate at the top of the convective zone, M_t the surface evaporative flux, q_c the water vapor mixing ratio within the cloud, and z_b and z_t the base and top of the cumulus cloud, respectively. The eddy vapor diffusion coefficient k_z' is determined in the same manner as k_z, assuming that $k_z' \approx k_z$ at the tropopause. The parameterization expression for convection, along with detailed meanings of each term, will be discussed in the next section.

2c. Surface Albedo Parameterization

To incorporate the ice-abledo feedback in the context of a one-dimensional climate model, it appears appropriate to express the surface albedo in terms of the surface temperature T_s in the form

$$r_s = r_{s,0} + \left(\frac{\partial r_s}{\partial T_s}\right)(T_s - T_{s,0}) \quad (6)$$

where $r_{s,0}$ and $T_{s,0}$ represent the mean annual surface albedo and surface temperature for the present condition, respectively, and $\partial r_s/\partial T_s$ denotes the albedo slope with respect to the surface temperature. On the basis of the study by Wang and Stone [1980], who utilized a two-mode Legendre polynomial expansion to relate the surface temperature and solar insolation, the

slope $\partial r_s/\partial T_s$ may be expressed as a function of the ice line directly and the surface temperature indirectly. In accord with their parameterization and consistent with the present one-dimensional model the surface albedo is expressed by

$$r_s = [a_2 (1 - x_s) + a_1 x_s] + S_2 (a_2 - a_1) (x_s - x_s^3) / 2 \quad (7)$$

where a_2 and a_1 are empirical constants associated with the ice-covered and ice-clear albedo values, S_2 denotes the coefficient for solar insolation as a function of latitude, and x_s is the sine of the latitude of the ice line position, which is correlated with the average surface temperature in the form

$$x_s = (0.6035 + 0.02078\ T_s)^{1/2} \quad (8)$$

with T_s in °C. Since (8) is an approximation, in the event that $x_s > 1$ in numerical calculations we set $x_s = 1$. In our present model, a_1 and a_2 are to be taken to be 0.118 and 0.55 so that the surface albedo for the present condition r_s of 0.13 is matched with the ice line position x_s of 0.95.

3. Parameterization of Cumulus Convection

It has been well known that a significant portion of the large-scale disturbances in the tropical atmosphere are driven by the latent heat release that takes place primarily in deep cumulus towers. Since the horizontal scale of these cumulus clouds is much smaller than the grid scale employed in representing the large-scale flows, the small-scale convective activities can only be incorporated in the large-scale equations through parameterization. Pioneering work on the parameterization of cumulus convection has been proposed by Kuo [1965, 1974], Ooyama [1971], Arakawa and Schubert [1974], and more recently by Anthes [1977]. In line with the one-dimensional climate model and consistent with the vertical transport parameterization described in section 2, we have followed and simplified the cumulus parameterization procedure described by Anthes.

The large-scale humidity transport may be described by the following equation:

$$\frac{\partial \bar{q}}{\partial t} + \nabla \cdot \bar{\mathbf{V}}\,\bar{q} + \frac{\partial(\rho\,\bar{w}\,\bar{q})}{\partial z} = -(\eta\, Q_c/L) - \frac{\partial(\rho\,\overline{w'q'})}{\partial z} \quad (9)$$

where Q_c is the rate of the latent heat release due to condensation and η denotes the fraction of convection within a grid cell. In order to incorporate the water transport in the one-dimensional, steady state climate model described in the foregoing section we set $\partial\bar{q}/\partial t = \nabla \cdot \bar{\mathbf{V}}\,\bar{q} = 0$, so that (9) becomes

$$\frac{\partial(\rho\,\bar{w}\,\bar{q})}{\partial z} + \frac{\partial(\rho\,\overline{w'q'})}{\partial z} = -\eta\, Q_c/L \quad (10)$$

Although (9) was written specifically for the evaluation of the water vapor distribution in a mesoscale environment, the mean quantities denoted in (10) may be thought of as some horizontally averaged value on a planetary scale. In this context it is appropriate to assume that the mean velocity $\bar{w}$ is so small that it can be neglected. Thus (10) is further reduced to

$$\frac{\partial(\rho\,\overline{w'q'})}{\partial z} = -\eta\, Q_c/L \quad (11)$$

Here, we have not considered an interactive evaporation of cloud and rain water that may contribute significantly to the moisture content in the atmosphere. However, in line with the one-dimensional model we utilize the climatological humidity profile proposed by Manabe and Wetherald [1967] in the form

$$h(z) = h(0) \left[\frac{p(z)/p(0) - 0.02}{0.98}\right] \quad (12)$$

While a prescribed relative humidity profile is extremely simplified from the point of view of the complete hydrological cycle, it does approximately account for the humidity change due to evaporation and precipitation processes (see, e.g., Hummel and Kuhn, 1981). This simplification also takes into account the fact that the incorporation of cumulus convection in climate models cannot be very elaborate, since the prime objective is to investigate the temperature perturbation. For cumulus convection to take place in the atmosphere a positive vertical moisture flux at the assumed base of the convection zone and a conditionally unstable temperature profile must be satisfied. Assuming that these two conditions exist in a synthetic atmosphere, we then proceed to model the cumulus convection on the basis of the conservation of moist static energy and water vapor mass for a rising parcel. We do so by dividing the one-dimensional troposphere into convective and nonconvective zones. In reference to Figure 1, within the cumulus convective column a constant air mass flow rate M is assumed since we have neglected the entrainment. Furthermore, since we also neglected the large-scale moistening effect by cumulus convection,

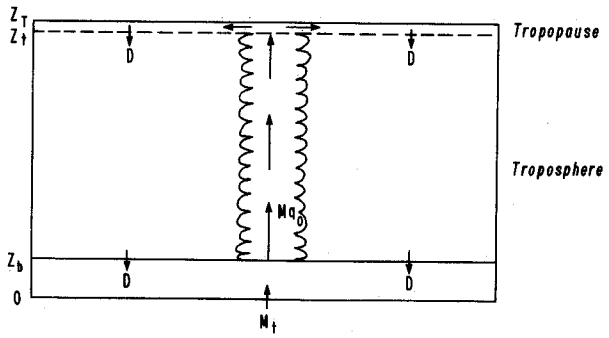

Fig. 1. The one-dimensional cumulus convection model. The troposphere is divided into cumulus convection and nonconvection zones. In the cumulus convection zone a constant air mass flow M is directed upward. D represents the constant environmental subsidence rate. Both M and D are area averaged values and are balanced exactly. Their associated water vapor mass fluxes are balanced by the surface evaporative flux M_t.

we set the moistening factor to zero. Subject to the aforementioned conditions, we may write Anthes, 1977, equations (26) and (39)]

$$-\int_{z_b}^{z_t} \eta\,\rho\,w_c\,\frac{\partial q_c}{\partial z}\,dz \approx \langle \eta\,\rho\,w_c\rangle\,[q_c(z_b) - q_c(z_t)] = M_t \tag{13}$$

where w_c denotes the vertical velocity within the cloud, q_c the water vapor mixing ratio within the cloud, and z_b and z_t the base and top of the cumulus cloud, respectively. It follows that

$$M = \langle \eta\,\rho\,w_c\rangle = \frac{M_t}{q_c(z_b) - q_c(z_t)} \tag{14}$$

where $\langle\ \rangle$ represents some vertically averaged value and M_t represents the surface evaporative flux derived from the surface flux parameterization.

In accordance with Anthes' parameterization, $\overline{w'q'}$, denoted in (11) may be expressed by

$$\overline{w'q'} = \eta\,\overline{(w_c - \bar{w})\,(q_c - \bar{q})}^{c} + (1-\eta)\,\overline{(w_0 - \bar{w})\,(q_0 - \bar{q})}^{0} \tag{15}$$

where w_0 and q_0 are the vertical velocity and mixing ratio, respectively, in the nonconvective region. With the assumption that $\bar{w} = 0$ we may rewrite (15) in the form

$$\overline{w'q'} = \eta\,w_c\,q_c + (1-\eta)\,w_0\,q_0 - [\eta\,w_c + (1-\eta)\,w_0]\,\bar{q}_0 \tag{16}$$

Moreover, $\eta\,w_c + (1-\eta)\,w_0 \equiv \bar{w} = 0$. Thus if we let $D = -(1-\eta)\,w_0\,q_0$ and $M = \eta\,\rho\,w_c$, we get

$$\rho\,\overline{w'q'} = M\,q_c(z) - D \tag{17}$$

Furthermore, substituting (14) into (17) yields

$$\rho\,\overline{w'q'} = \frac{M_t\,q_c(z)}{q_c(z_b) - q_c(z_t)} - D \tag{18}$$

In order to obtain the saturation water vapor mixing ratio within the cloud the cloud temperature needs to be calculated from the conserved quantity. It is assumed that the moist static energy $E(z) = C_pT + gz + Lq$ for a parcel under moist adiabatic lifting in cloudy regions is conserved, i.e., $dE(z)/dz = 0$. Furthermore, assuming that the humidity within the rising parcel is saturated, we then obtain the following relationships via the Clausius-Clapeyron equation in the forms

$$E(z_b) = C_pT_c + gz + Lq_c \tag{19}$$

$$q_c = q_s(T_c) = \frac{\varepsilon P_w^*}{P_a}\exp\left[-\frac{L}{\tilde{R}}\left(\frac{1}{T^*} - \frac{1}{T_c}\right)\right] \tag{20}$$

where $E(z_b)$ is the moist static energy at the cloud base; T_c and q_c represent the cloud temperature and water vapor mixing ratio, respectively; P_w^* is the saturated water vapor pressure at a reference temperature T^*; P_a is the air pressure; and $\tilde{R}$ is the gas constant for water vapor. It follows that once the atmospheric temperature and humidity profiles are given the temperature and humidity within the cloud, the vertical mass flow rate M, detrainment rate D and the humidity eddy flux can be determined through (14) - (18).

In order for the cumulus convection to take place the buoyancy force must be positive so that virtual temperature in the cloud region $T_{v,c}$ is greater than that in the clear region $T_{v,0}$. In accordance with Arakawa and Schubert [1974] it can be shown that

$$T_{v,c} - T_{v,0} \approx \frac{1}{C_p + L(\partial q^*/\partial T)}\,(E_c - E_0^*) \tag{21}$$

where q^* denotes the saturation water vapor mixing ratio, and E_c and E_0^* represent the moist static energy for the cloud and the clear column under saturation conditions, respectively. Since $\partial q^*/\partial T > 0$, an alternative criterion for cumulus convection to occur may be obtained from testing whether E_c is greater than E_0^* at the cloud base z_b. Once the convection has taken place, the rising motion will reach a certain height at which the kinetic energy of the parcel $K(z_t) \to 0$. According to Anthes [1977], the kinetic energy may be obtained from the following equation:

$$\frac{dK}{dz} = \frac{g(T_{v,c} - T_{v,0})}{(1+\alpha)\,T_{v,c}} \tag{22}$$

where α is the vertical mass coefficient that compensates for the neglect of nonhydrostatic pressure perturbations. Once the kinetic energy is known, the vertical velocity within the cloud is given by

$$w_c = (2\,K)^{1/2} \tag{23}$$

and the fraction of convection within a grid cell is [Anthes, 1977]

$$\eta = \frac{M}{\rho w_c} \tag{24}$$

It should be noted that, since the effects of entrainment and precipitation processes have been neglected for simplicity in this study, the computed kinetic energy and vertical velocity within the cloud will tend to be larger. Typical vertical velocity and fractional cumulus cloud coverage calculated in the model are on the order of 10 m s^{-1} and 10^{-3}, respectively. However, the present parameterization for cumulus convection within the context of climatic temperature perturbation experiments, appears to be physically adequate, at least for the physical understanding of the relative importance of cumulus convection associated with the radiative perturbation of internal and external climatic components.

As pointed out in the introduction, Lindzen

et al. [1982], in their pioneering paper, have also developed a simple cumulus parameterization scheme for climatic temperature perturbation studies. Their method is basically concerned with the determination of convective heating rate by using a dry static energy profile and an assumed drag coefficient for the surface evaporation. In addition, no criteria has been devised for the onset of convection. It is evident, however, that the aforementioned scheme incorporates moist static energy in the development of convection and provides a criteria for cumulus convection to take place.

4. Results and Discussion

In the present perturbation study, two types of temperature profiles were used for reference purposes. These include standard and tropical temperature profiles (Figure 2). The standard temperature profiles in this figure are the U.S. standard profile and results compiled by Oort and Rasmusson [1971] for the northern hemisphere. In addition, three surface relative humidity values h(0) of 0.7, 0.8, and 0.9 are utilized to generate relative humidity profiles according to (12).

Figure 3a illustrates the convective heating rate profile for tropical and U.S. standard atmospheres by using h(0) of 0.9. The vertical distribution of heating shows a pronounced convection effect in the tropical atmosphere but a limited response in the standard atmosphere. In this presentation we have combined the heating due to large-scale eddy transport in the nonconvective zone with the cumulus convective heating. The extent of condensational heating due to cumulus convection appears to be determined by the depth of the conditionally unstable layer, the depth of the positive buoyancy region, and the total amount of buoyancy force generated by the excessive cloud temperature relative to the temperature of the surrounding area. In fact in Kuo's [1974] scheme the vertical distribution of heating is determined by the normalized value of $(T_{v,c} - T_{v,0})$. Also, we have found that the presence of conditional instability in a vertical zone alone is not sufficient to generate cumulus convection, since a positive buoyancy force may not exist due to the dryness of the surrounding area.

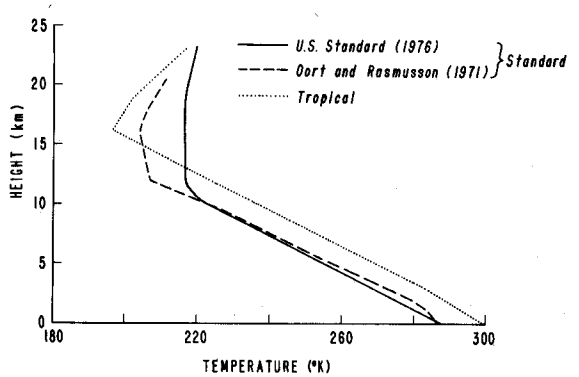

Fig. 2. Temperature profiles for standard (global) and tropical conditions.

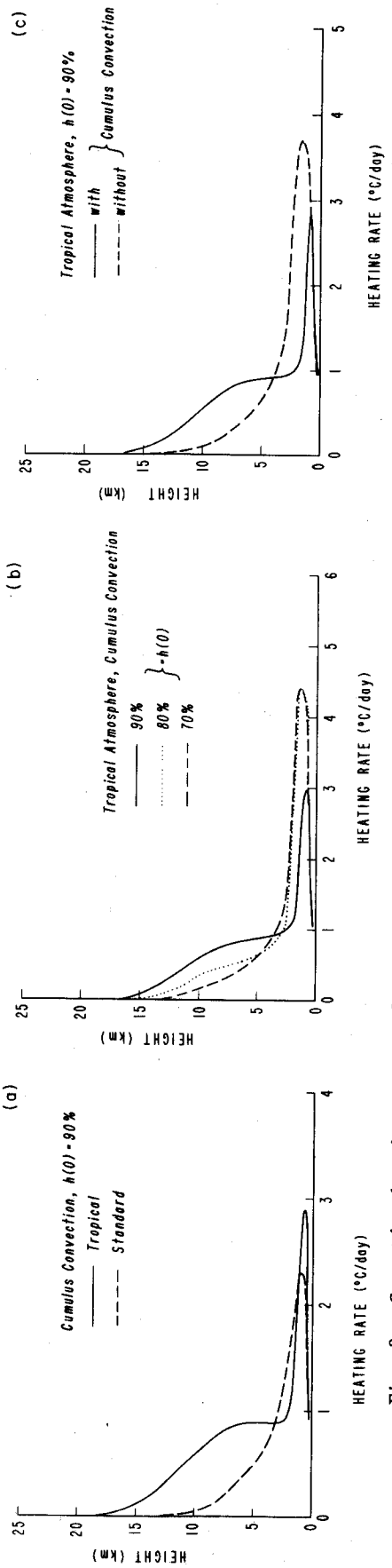

Fig. 3. Covective heating rate profiles produced by the present cumulus convection model for (a) tropical and U.S. standard atmospheres, both with h(0) = 0.9; (b) tropical atmosphere with h(0) = 0.9, 0.8, and 0.7; and (c) tropical atmosphere with and without the incorporation of cumulus parameterization.

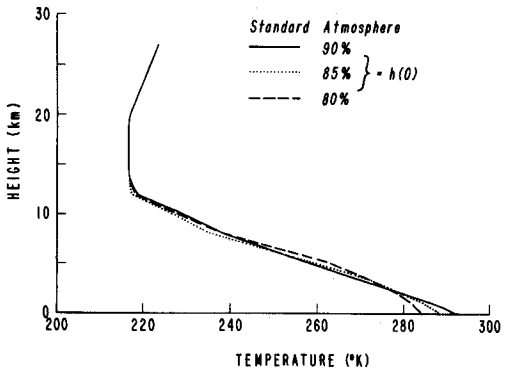

Fig. 4. Equilibrium temperature profiles corresponding to mean annual global conditions based on three relative humidity profiles with h(0) = 0.9, 0.85, and 0.8.

For the tropical atmosphere, however, even when the surface humidity is as low as 70%, there is always a zone of positive buoyancy force. This allows us to study the effects of cumulus convection based on three surface relative humidities on the atmospheric heating rate by using the same temperature profile (Figure 3b). For high surface humidity conditions there would be a larger possibility for cumulus convection to take place. This will result in the shift of the heating rate distribution toward the upper part of the atmosphere. Thus the surface humidity is a major parameter in determining the vertical profile of condensational heating as well as whether cumulus convection will occur.

The next aspect to be examined is the extent of vertical shifting of the condensational heating. Figure 3c shows the heating rate profiles obtained with and without cumulus parameterization for a tropical atmosphere with 90% surface relative humidity. Below 5 km the heating based on the K theory without the incorporation of cumulus parameterization is larger than that with the inclusion of cumulus parameterization, while the reverse is true for all levels above 5 km. The total integrated heating for the vertical column is the same for both cases, however. It is noted that cumulus convection generates large vertical velocity in cloud regions, which will significantly enhance the rate of condensation, especially in upper levels. Although the fraction of cumulus clouds represents only a very small portion of the entire horizontal grid cell, the latent heat release in this small region generates significant large-scale heating effects, especially in the upper part of the atmosphere.

In radiative-turbulent equilibrium calculations we have prescribed the height, thickness, and fractional coverage for six cloud types presented by Liou and Ou [1983]. Carbon dioxide concentration is taken to be 330 ppm, corresponding to the present condition. For infrared calculations, all clouds except cirrus are assumed black. The cirrus emissivity, transmissivity, and reflectivity are set to be 0.47, 0.53, and 0.073, respectively, as presented by Liou and Ou. In the solar part, cloud radiative properties are calculated according to parameterization equations developed by Liou and Wittman [1979]. The solar constant S and average cosine of the solar zenith angle μ_0 are taken to be 1360 W/m^2 and 0.5, respectively. The duration of sunlight is 12 hours for mean annual conditions.

Figure 4 depicts equilibrium temperature profiles corresponding to three relative humidity profiles. The temperature profile corresponding to h(0) = 0.85 appears to agree most closely with that given by Oort and Rasmusson (1971; see our Figure 2) in most of the troposphere, with a difference of no more than 2°K below 10 km. Both sets of results show a smaller lapse rate near the surface but a larger lapse rate (close to adiabatic lapse rate) in the upper troposphere as compared to 6.5°C/km which is typical of the U.S. standard temperature profile depicted in Figure 2. The smaller lapse rate near the surface is due to the enhanced eddy sensible heat transport from the surface to the atmosphere above. Close to and below the tropopause, however, both latent and sensible turbulent heat exchanges are quite small, so that the lapse rate is basically determined by radiative equilibrium. Table 1 depicts the equilibrium water vapor mixing ratio computed from the present model. Also shown for comparisons are the climatological values listed in Oort and Rasmusson. Our humidity values are somewhat higher between the 950- and 700-mbar levels because of higher equilibrium temperatures derived from the model.

Figure 5 shows heating rate profiles due to net radiative cooling, latent heat release, and eddy sensible heat transport for cases with and without the incorporation of cumulus parameterization by using h(0) = 0.9. Since these profiles are determined from the balance between various components involving radiative absorption and emission and latent and sensible heat transport, which are all directly related to temperature, it is difficult to pinpoint processes corresponding to forcing and responses. However, in the context of the thermodynamic energy balance, the rate of heating due to eddy sensible heat and latent heat release should be exactly balanced by the rate of cooling by radiative transfer. This balance is evident in Figure 5. With respect to the effect of incorporating cumulus convection it is seen that this process generates larger heating rates in the region between 6 and 13 km at the expense of heating in the lower region from 2 to 5 km. The maximum heating rate difference with and without the in-

TABLE 1. Water Vapor Mixing Ratio Profile [h(0) = 85%]

Pressure mb	Oort & Rasmusson [1971] g/kg	Present Model g/kg
1000	10.5	10.6
950	9.1	9.9
900	7.7	9.0
850	6.4	8.0
700	3.5	4.7
500	1.2	1.2
400	0.6	0.4
300	0.2	0.1

clusion of cumulus convection is about 0.4°K/d at ~8 km. Consistent with the heating profile produced by cumulus convection, the radiative cooling profile shows a similar pattern. It is also noted that above ~5 km sensible heat exchanges are practically insignificant. Thus radiative cooling in this region is basically balanced by latent heat release.

Vertical profiles of temperature changes due to doubling of CO_2 concentration for two humidity profiles, h(0) = 0.85 and 0.9, with and without cumulus parameterization are illustrated in Figure 6. For the case of h(0) = 0.9 without cumulus convection, temperatures increased up to ~15 km due to the CO_2-induced greenhouse effect, with a maximum increase located at the surface. On the contrary, above ~15 km, temperature decreases, and the magnitude of these decreases increase with height, which is a result of IR emission to space by CO_2. With the incorporation of cumulus convection, because more latent heat release is shifted upward, the temperature change below ~4 km is reduced, while above this height the temperature change is increased, with the maximum of 2.8°C located at ~8 km. The surface temperature response was reduced by ~0.8°C in this sensitivity study. For h(0) = 0.85, which closely represents the mean annual humidity condition, the criterion for invoking cumulus parameterization is not satisfied in the present condition. While cumulus convection will take place when CO_2 concentration is doubled, the region of cumulus convection is quite limited (between 5-8 km). As a result the effect of incorporating cumulus parameterization is not so apparent as in the case of h(0) = 0.9. Nevertheless there is a slight decrease in temperature change below ~6 km, coupled with a slight rise of sensitivity between 6 and 8 km in the case of doubling of CO_2. In this case, surface temperature change with the incorporation of cumulus convection appears to be insignificant.

Table 2 shows a summary of results obtained from a number of numerical sensitivity experiments based on three relative humidities for mean annual global conditions with respect to present and doubled CO_2 concentrations. The case when

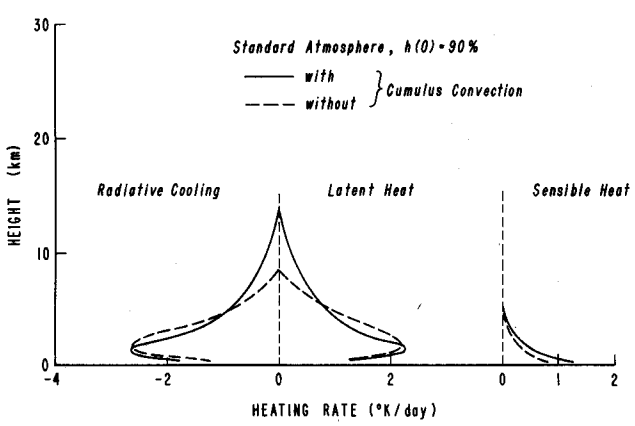

Fig. 5. Heating rate profiles due to radiative cooling, latent heat release, and eddy sensible heat transport corresponding to mean annual global conditions for h(0) = 0.9 with and without the incorporation of cumulus parameterizations.

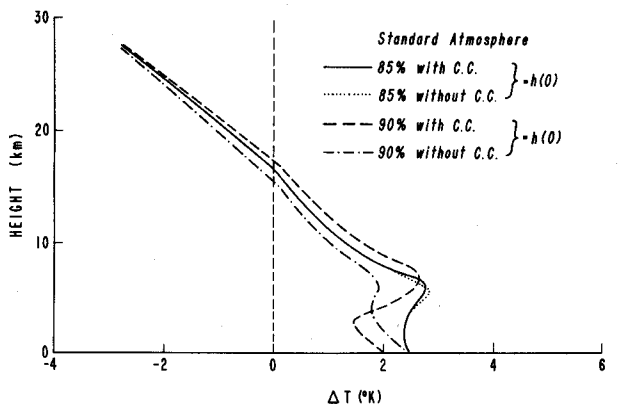

Fig. 6. Vertical profiles of temperature changes due to doubling of CO_2 for two humidity profiles, h(0) = 0.85 and 0.9, with and without cumulus parameterization.

the surface humidity is 85% gives a surface temperature closest to the climatological mean (288.1°K). It is clear from these results that the equilibrium surface temperature increases with the surface humidity. A ±5% change of surface humidity resulted in a surface temperature change of ~±4°K. This surface temperature sensitivity is primarily caused by the humidity feedback. Different surface relative humidities also give different surface temperature changes in cases associated with doubling of CO_2. As shown in Table 2 we find ΔT_s = 2.07, 2.41, and 1.79°K, corresponding to h(0) = 0.9, 0.85, and 0.8, respectively. The case when h(0) = 0.85 generates the highest sensitivity. This is because for a higher surface relative humidity, stronger convection will reduce the surface temperature sensitivity in perturbation experiments. Moreover, for lower surface relative humidity, less humidity feedback also leads to a reduction of sensitivity because the greenhouse effects are decreased. In addition we notice that for the 90% humidity case the surface albedo is invariably 0.118. Thus there will be no albedo feedback, leading to a decrease of the sensitivity of temperature variations due to doubling of CO_2.

Table 2 also depicts the resulting surface energy budget components. The computed surface latent heat flux LM_t ranges from 83.8 to 85.8 W/m^2, which compares favorably with the climatology values of 88 W/m^2 presented by Budyko [1982]. The corresponding evaporation rate M_t, ranging from 105.3 to 107.5 cm/yr, again compares well with estimated values of 98.1 and 109.7 cm/yr provided by Sellers [1965] and Budyko [1982], respectively. The surface latent heat flux does not vary significantly with different humidity profiles. However, decreasing relative humidity causes increasing evaporation as the vertical humidity gradient near the surface becomes larger. The solar flux absorbed at the surface also changes insignificantly (158.9-157.5 W/m^2) with humidity, but the net IR emission varies somewhat (58.8-55.5 W/m^2). The net absorbed radiative flux (100.1-102.0 W/m^2), which should be equal to the total latent plus sensible heat fluxes, is somewhat smaller than the estimated value of 105 W/m^2 given by Budyko. At the top of the atmosphere the outgoing emitted IR

TABLE 2. A Summary of Results Obtained From a Number of Sensitivity Experiments Based on Three Surface Relative Humidities for Mean Annual Global Conditions.

h(0)	CO_2	T_s °K	r_s	x_s	H_s W/m^2	LM_t W/m^2	H W/m^2	$F_S(0)$ W/m^2	$F_{IR}(0)$ W/m^2	$F_{IR}(\infty)$ W/m^2	M_t cm/yr
0.9	1 x CO_2 (C*)	292.45	0.118	1.000	16.3	83.8	100.1	158.9	58.8	239.8	105.3
	1 x CO_2 (nc†)	293.15	0.118	1.000	17.5	84.7	102.2	158.4	56.2	239.7	106.4
	2 x CO_2 (C)	294.52	0.118	1.000	17.9	86.2	104.1	157.9	53.8	240.5	108.0
	2 x CO_2 (nc)	295.67	0.118	1.000	18.7	87.3	106.0	157.4	51.4	240.3	109.7
0.85	1 x CO_2 (nc)	288.48	0.127	0.962	16.4	85.5	101.9	158.2	56.3	238.7	107.1
	2 x CO_2 (C)	290.89	0.121	0.988	19.0	87.8	106.8	158.1	51.3	240.2	110.0
	2 x CO_2 (nc)	290.89	0.121	0.988	19.0	87.8	106.8	158.1	51.3	240.2	110.0
0.8	1 x CO_2 (nc)	284.48	0.138	0.918	16.2	85.8	102.0	157.5	55.5	237.2	107.5
	2 x CO_2 (nc)	286.27	0.133	0.938	18.4	87.1	105.5	157.4	51.9	238.6	109.1

*C, with cumulus parameteriation.
†nc, without cumulus parameterization.

flux, which is balanced by the absorbed solar flux, decreases with decreasing humidity (238.8-237.2 W/m^2). Compared to satellite observed values of 232 and 237 W/m^2 presented by Stephens et al. [1981] and Vonder Haar and Suomi [1971], respectively, the present values are somewhat higher. Finally, perturbation results with and without the inclusion of cumulus parameterization for cases of h(0) = 0.9 and h(0) = 0.85 are discussed. For h(0) = 0.85 involving doubled CO_2 concentration, although the criteria for cumulus convection is satisfied, the extent of convection is limited. Consequently, results with and without cumulus parameterizations are almost identical. In the case of h(0) = 0.9, when CO_2 concentration is doubled, with and without the incorporation of cumulus convection, surface temperature increases are 2.07° and 2.52°K, respectively. Clearly, the smaller sensitivity in the cases involving cumulus parameterization is due to the stronger convection simulated in the model.

It is recognized that deep cumulus towers generally occur in the tropical ITCZ regions. Although in a global one-dimensional model it is physically impossible to specify the position of cumulus convection, we may apply such a model, however, to a locality where cumulus convection is most active. In order to do so, it is necessary to modify the model to allow horizontal transport so that the equilibrium temperature may be derived from the energy balance consideration. Considering a latitude-height column of the atmosphere, equilibrium temperatures are the result of the energy balance between the net downward solar flux and upward IR flux, vertical eddy heat flux, divergence of meridional sensible and latent heat fluxes due to atmospheric motions, and divergence of meridional sensible heat fluxes due to ocean currents. Thus we modify the energy balance by replacing $F_S(z)$ on the right side of equation (1) with $F_S(z) - F_H(z) - R$, where $F_H(z)$ is the integrated divergence of atmospheric meridional sensible and latent heat fluxes between the surface and height z, and R is the corresponding oceanic transport term equal to the net downward heat flux into the ocean, based on the surface energy budget. The latter term is prescribed in accordance with the climatological data provided by Sellers [1965]. In addition we consider a tropical zone from 0° to 10°N and prescribe the mean annual meridional circulation from the data compiled by Oort and Rasmusson [1971] to compute $F_H(z)$. Both the atmospheric and oceanic transport fluxes are fixed in the numerical sensitivity experiments. With the horizontal transport flux incorporated in the one-dimensional model, we then utilized a cosine of the solar zenith angle of 0.6, a 12-hour sunlight duration, and a surface albedo of 0.06 in the calculation to represent the mean annual condition for tropical atmospheres. Moreover, the surface relative humidity is chosen to be 80% in line with the climatological value reported by Oort and Rasmusson.

Figure 7 shows the equilibrium temperatures for the tropical atmosphere derived from the modified one-dimensional model with and without the incorporation of cumulus convection. Also depicted for comparison is the climatological tropical temperature profile corresponding to 0-10°N taken from data compiled by Oort and Rasumsson [1971]. With the incorporation of cumulus convection, equilibrium temperatures below 8 km are reduced by about 2-3°K when they are compared with those without the inclusion of cumulus convection. The reverse is true for the atmosphere from 8 to 25 km. The temperature profile in the troposphere generated by the present one-dimensional model with fixed horizontal fluxes agrees closely with that provided by Oort and Rasmusson within about 1°K. This good agreement is quite encouraging.

Finally, we study sensitivity of CO_2 doubling on equilibrium temperatures with and without cumulus convection included in the experiment under tropical conditions. As shown in Figure 8, without the incorporation of cumulus convection the maximum temperature increase occurs at the surface with a ΔT of 4.3°K. The temperature increase due to CO_2 doubling in the tropical atmosphere spreads to a larger vertical region (0-20 km) than that in the standard atmosphere (0-15 km). Furthermore, without the introduction of cumulus convection the surface temperature increase in the tropics is much larger than that in the standard atmosphere under global conditions by a factor of about 2. This large increase is evidently caused by the enhanced humidity feedback in the tropics. When cumulus convection is included in the model a significant shift of the temperature increase due to CO_2 doubling is quite apparent. The surface temperature increase reduces from 4.3 to 2.5°K. This reduction is compensated for by the pronounced increase of ΔT in the upper troposphere and lower stratosphere. A maximum of about 4°K is seen at a level of about 15 km.

In light of the preceding results, it is appropriate to conclude that the influence of cumulus convection on the climatic temperature perturbation appears to be extremely significant in the tropics for mean annual conditions. It is quite clear that the full solution to the effects of cumulus convection on climatic temperature perturbations requires at least a two-dimensional model in which the latitudinal dependence of heating rates due to cumulus convection and its interactions with mean circulation and horizontal eddy transports of sensible and latent heat fluxes can be simulated and quantitatively evaluated.

5. Conclusions

In this paper the one-dimensional radiative-turbulent model proposed by Liou and Ou [1983] based on the principle of thermodynamic energy balance has been modified and refined. These modifications and refinements include surface flux parameterization utilizing climatology data and evaporation physics, the inclusion of a cumulus parameterization for the vertical transport, and parameterization of the one-dimensional surface albedo feedback. The cumulus parameterization used in the present study is basically a Kuo-type scheme described and modified by Anthes [1977]. The vertical distribution of condensational heating is determined by virtue of the air and water vapor mass balance. Moreover, utilizing the surface relative humidity and the vertical profile of moist static energy, the criteria for cumulus convection to take place is derived with respect to the one-dimensional radiative-turbulent model.

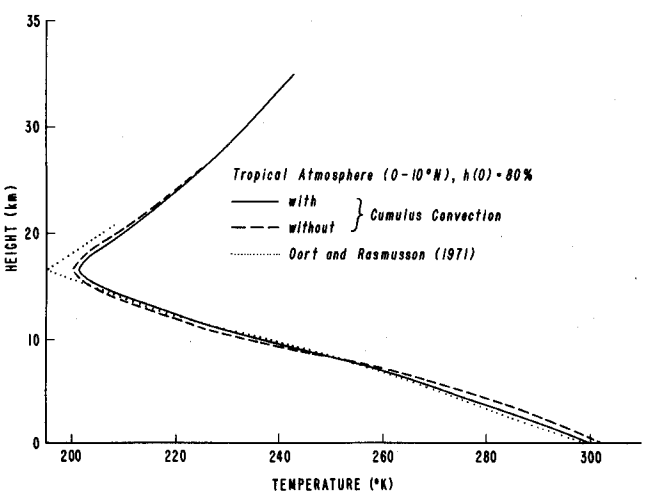

Fig. 7. Equilibrium temperature profiles in a tropical atmosphere for h(0) = 0.8 with and without the incorporation of cumulus parameterization. Also depicted for comparison is the climatological temperature profile for 0-10°N compiled by Oort and Rasmusson [1971].

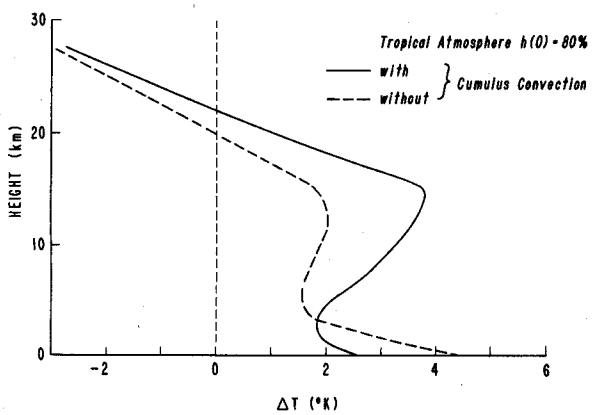

Fig. 8 Vertical profiles of temperature changes due to doubling of CO_2 for h(0) = 0.8 with and without the incorporation of cumulus parameterization.

A series of numerical experiments were undertaken to understand the physical behavior of the present cumulus convection sheme in terms of the condensational heating rate profile. First, we found that the extent of condensational heating due to cumulus convection appears to be determined by the depth of the conditionally unstable layer and the total amount of buoyancy force generated by the excessive cloud temperature over the surrounding temperature. This is evidenced by a significant upward shift of the heating rate distribution when using the tropical temperature profile. However, little upward shifting is seen when using the U.S. standard temperature profile.

Furthermore, utilizing the one-dimensional radiative-turbulent model with the incorporation of cumulus parameterization, we found that an atmosphere with a higher relative humidity will generate a higher temperature near the surface. In addition, in the upper part of the troposphere the temperature lapse rate increases as convective heat exchanges decrease so that the temperature profile gradually approaches that corresponding to pure radiative equilibrium. Also, a higher surface relative humidity will produce a large upward shift of the equilibrium condensational heating rate. This leads to an increase in radiative cooling due to the temperature increase required by the thermodynamic energy balance under equilibrium conditions.

The model-generated climate sensitivity due to doubling of CO_2 reveals that the surface temperature increase ΔT_S varies with the surface relative

humidity. For h(0) = 0.9, 0.85, and 0.8, ΔT_s are 2.07, 2.41, and 1.79°K, respectively. For the case of h(0) = 0.9, if cumulus convection is not included, ΔT_s is found to be 2.52°K. Activities of cumulus convection lead to the reduction of the temperature change in the lower troposphere. Such a reduction is compensated for by the increase of temperature sensitivity in higher levels of the troposphere. For the case when h(0) = 0.85, which corresponds closely to the mean annual humidity value, the sensitivity of cumulus convection on the surface temperature perturbation is not apparent in the one-dimensional global model experiment.

Finally, by fixing the large-scale horizontal transports of sensible and latent heat fluxes, we have also carried out numerical experiments for the equilibrium temperature and its perturbations in the tropical atmosphere. Employing a surface relative humidity of 80%, and with the incorporation of cumulus convection along with other mean annual parameters, we show that the model-derived equilibrium temperature profile closely agrees with that for the mean annual condition. Sensitivity experiments involving the doubling of CO_2 show that the surface temperature increase reduces from 4.3 to 2.5°K when interactive cumulus convection is included in the calculation. These experiments also illustrate a large temperature increase at the top level of cumulus towers. It is quite evident that the effects of cumulus convection on climatic temperature perturbations due to variations in radiative components appear to be extremely significant in the tropics. Thus investigation of the extent and degree of these effects in an annual mode on mid and high latitudes requires a two-dimensional model in which the latitudinal dependence of heating rates and various dynamic feedbacks can be numerically evaluated.

Acknowledgements. This research has been supported by the Division of Atmospheric Sciences, National Science Foundation, under grant ATM81-09050 and in part by the Air Force Geophysics Laboratory under contract F19628-83-K-0015. Sharon Bennett typed and edited several versions of the manuscript.

References

Albrecht, B. A., A cumulus parameterization for climate studies of the tropical atmosphere, 1, Model formulation and sensitivity tests, J. Atmos. Sci., 40, 2166-2182, 1983.

Anthes, R. A., A cumulus parameterization scheme utilizing a one-dimensional cloud model, Mon. Weather Rev., 105, 270-286, 1977.

Arakawa, A., and W. H. Schubert, Interaction of a cumulus cloud ensemble with the large-scale environment, 1, J. Atmos. Sci., 31, 674-701, 1974.

Budyko, M. I., The Earth's Climate: Past and Future, 307 pp., Academic, New York, 1982.

Deardorff, J. W., The counter-gradient heat flux in the lower atmosphere and in the laboratory, J. Atmos. Sci., 23, 503-506, 1966.

Donner, L. J., H-L. Kuo, and E. J. Pitcher, The significance of thermodynamic forcing by cumulus convection in a general circulation model. J. Atmos. Sci., 29, 2159-2181, 1982.

Hummel, J. R., and W. R. Kuhn, An atmospheric radiative-convective model with interactive water vapor transport and cloud development, Tellus, 33, 372-381, 1981.

Kuo, H-L., On formation and intensification of tropical cyclones through latent heat release by cumulus convection, J. Atmos. Sci., 22, 40-63, 1965.

Kuo, H-L., Further studies of the parameterization of the influence of cumulus convection on large-scale flow, J. Atmos. Sci., 31, 1232-1240, 1974.

Lindzen, R. S., A. Y. Hou, and B. F. Farrell, The role of convective model choice in calculating the climate impact of doubling CO_2, J. Atmos. Sci., 39, 1189-1205, 1982.

Liou, K. N., and S. S. Ou, Theory of equilibrium temperature in radiative-turbulent atmospheres, J. Atmos. Sci., 40, 215-229, 1983.

Liou, K. N., and G. D. Wittman, Parameterization of the radiative properties of clouds, J. Atmos. Sci., 36, 1261-1273, 1979.

Manabe, S., and R. Strickler, Thermal equilibrium of the atmosphere with a convective adjustment, J. Atmos. Sci., 21, 361-385, 1964.

Manabe, S., and R. T. Wetherald, Thermal equilibrium of the atmosphere with a given distribution of relative humidity. J. Atmos. Sci., 24, 241-259, 1967.

Oort, A. H., and E. M. Rasmusson, Atmospheric Circulation Statistics, NOAA Prof. Pap. 5, 323 pp., U.S. Dept. Commer., Washington, D.C., 1971.

Ooyama, K., A theory of parameterization of cumulus convection, The Syono Memorial Volume, J. Meteorol. Soc. Jpn., 49, 744-756, 1971.

Ou, S. S., and K. N. Liou, Parameterization of carbon dioxide 15 μm absorption and emission, J. Geophys. Res., 88, 5203-5207, 1983.

Peng, L., M. D. Chou, and A. Arking, Climate studies with a multi-layer energy balance model, 1, Model description and sensitivity to the solar constant, J. Atmos. Sci., 39, 2639-2656, 1982.

Priestley, C. H. B., and R. J. Taylor, On the assessment of surface heat flux and evaporation using large-scale parameters, Mon. Weather Rev., 100, 81-92, 1972.

Sellers, W. D., Physical Climatology, 272 pp., The University of Chicago Press, Chicago, Ill., 1965.

Stephens, G. L., G. G. Campbell, and T. H. Vonder Haar, Earth radiation budgets, J. Geophys. Res., 86, 9739-9760, 1981.

Vonder Haar, T. H., and V. E. Suomi, Measurements of the earth's radiation budget from satellites during a five-year period, 1, Extended time and space means, J. Atmos. Sci., 28, 305-314, 1971.

Wang, W-C., and P. H. Stone, Effect of ice-albedo feedback on global sensitivity in a one-dimensional radiative-convective model, J. Atmos. Sci., 37, 545-552, 1980.

K. N. Liou and S-C. S. Ou, Department of Meteorology, University of Utah, Salt Lake City, UT 84112.

(Received May 14, 1984;
revised September 14, 1984;
accepted September 18, 1984.)